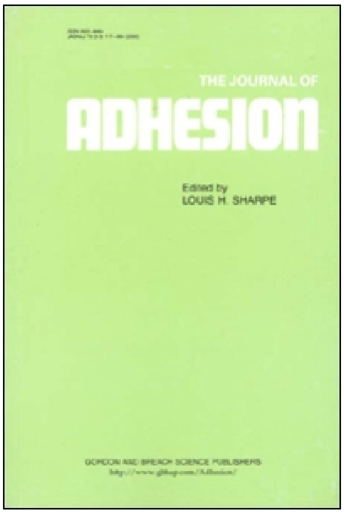

The Journal of Adhesion
Publication details, including instructions for authors and subscription information:
http://www.informaworld.com/smpp/title~content=t713453635

Wilhelmy Technique and Solidification Front Technique to Study the Wettability of Fibres

S. K. Li[a]; R. P. Smith[a]; A. W. Neumann[a]
[a] Department of Mechanical Engineering, University of Toronto, Toronto, Ontario, Canada

To cite this Article Li, S. K. , Smith, R. P. and Neumann, A. W.(1984) 'Wilhelmy Technique and Solidification Front Technique to Study the Wettability of Fibres', The Journal of Adhesion, 17: 2, 105 — 122
To link to this Article: DOI: 10.1080/00218468408079669
URL: http://dx.doi.org/10.1080/00218468408079669

J. Adhesion, 1984, Vol. 17, pp. 105–122
0021–8464/84/1702–0105 $18.50/0

Printed in the United Kingdom

Wilhelmy Technique and Solidification Front Technique to Study the Wettability of Fibres

S. K. LI, R. P. SMITH and A. W. NEUMANN

Department of Mechanical Engineering, University of Toronto, Toronto, Ontario, Canada M5S 1A4

(*Received July 18, 1983; in final form November 14, 1983*)

The strength of fibre-reinforced materials depends heavily on the adhesion between the fibre and the resin. To predict the bond strength of the adhesion, it is desirable for the surface tension of the fibre to be known. Two independent methods, the Wilhelmy balance method and the solidification front method, were investigated. The fibres used for this investigation included a carbon fibre, Thornel 300®, and an aromatic polyamide fibre, Kevlar®.

In the Wilhelmy experiments three liquids, ethylene glycol, glycerol and distilled water were employed to measure the surface tensions of the test fibres. They were found to be 42.4 mJ/m^2 and 43.7 mJ/m^2 for the carbon fibre and Kevlar, respectively. These values agreed very well with the results obtained from the solidification front method, from which the carbon fibre was found to have a surface tension value of 41.8 mJ/m^2 while that for Kevlar was 46.4 mJ/m^2. Furthermore, error analysis has shown that the error limits of the experiments are within 5% of the resulting values. The reproducibility and accuracy of these two techniques indicate that they are viable for determining the surface tension of small diameter fibres.

INTRODUCTION

The wettability of reinforcing fibres will be studied in this paper since this property has an effect on the fibre-resin bond strength in composite materials. The overall strength of a reinforced material depends heavily on how strong this bond is. Good adhesion is essential for the transfer of stresses and thus the strength of the composite material, while poor adhesion means a decrease in the composite tensile or compression strength or the lack of ability to maintain its normal strength on exposure to water under adverse conditions.[1]

An important condition for achieving a good adhesive bond between the fibre and the matrix resin is that the liquid resin has to wet the surface of the fibre to obtain complete and intimate contact. The theory of adhesion and its relationship with surface free energy and wetting has been studied by Sharpe *et al.*,[2] Huntsberger,[3] Zisman[4] and many other workers. It has been agreed by most of the workers that for the liquid resin to wet or spread on the fibre completely, the surface tension of the liquid resin must be less than that of the fibre itself. Therefore, in order to optimize the reinforcement of the composite material, it is necessary to know the solid surface tension of the fibre, and the surface tension of the liquid resin.

The conventional means of determining the wettability and surface tension of a solid is to perform contact angle measurements on a large smooth surface of the solid. Knowing the surface tension of the liquid used in this measurement allows for the calculation of the surface tension of the solid from the contact angle. However, when dealing with small diameter fibres this direct approach to determining contact angles and surface tensions is difficult.

Two independent techniques will be discussed and utilized to obtain contact angle and surface tension information for small diameter carbon and Kevlar fibres. Several workers have used the Wilhelmy technique to measure the wettability of fibres.[5,6,7,8] We will use the Wilhelmy[5,9] technique to determine the contact angles of various liquids on our test fibres. However, because of the sensitivity of these measurements to error, due to the small diameter of the fibres, a second independent technique was also employed. The newly developed solidification front technique provides an alternate means to obtain contact angle and surface tension data for these fibres. The correlation between the results obtained by these two methods will serve to check the validity of our approach.

EXPERIMENTAL METHODS

Two independent methods, the Wilhelmy balance method and the solidification front method, were used in this investigation. The fibres used for the study were: a high strengh, high modulus carbon fibre, the Thornel 300 carbon fibre from Union Carbide Corporation and an aromatic polyamide fibre, Kevlar from duPont de Nemours & Company.

The Wilhelmy balance method

When a solid, which is bounded by vertical surfaces, is partially immersed into a liquid, due to capillarity effects the liquid will either rise or be depressed along the vertical wall, thus exerting a force on the solid. The magnitude of the force, F, exerted on the plate by the liquid is

$$F = p\gamma_{LV}\cos\theta \qquad (1)$$

where p is the perimeter of the solid; γ_{LV} is the liquid surface tension and θ is the contact angle between the solid and the liquid.

Thus if the perimeter of the immersed fibre and the surface tension of the liquid are known, the contact angle between the fibre and the liquid matrix can be calculated by measuring the pulling force, F.

Apparatus and experimental outline

A schematic diagram of the apparatus used for the Wilhelmy balance method is shown in Figure 1. A section of the fibre (A), about 3 to 5 mm long, was glued to the end of a glass rod (B), with a diameter of about 0.5 mm. Because of the small dimension of the measured fibre, the process of gluing it to the glass rod had to be done under a Wild Leitz M5-Apo stereo-microscope. In this process, both the fibre and the glass rod were each held between two microscope slides laying on the microscope platform. A fast curing epoxy was then added to the tip of the glass rod and the fibre was brought into contact with the epoxy by manoeuvring the slides under the stereo-microscope. After the epoxy had cured, the slides were carefully removed. The glass rod, with the fibre at its tip, was then suspended from the electro-balance (Cahn R-H Electrobalance) (C). In order to protect the fibre against air convection during the experiment, a glass sleeve (D) was used to cover the hang-down arrangement. The liquid (E) used for the contact angle measurement was contained in a double-walled glass cell (F). A Teflon lid (G) with a small hole for the passage

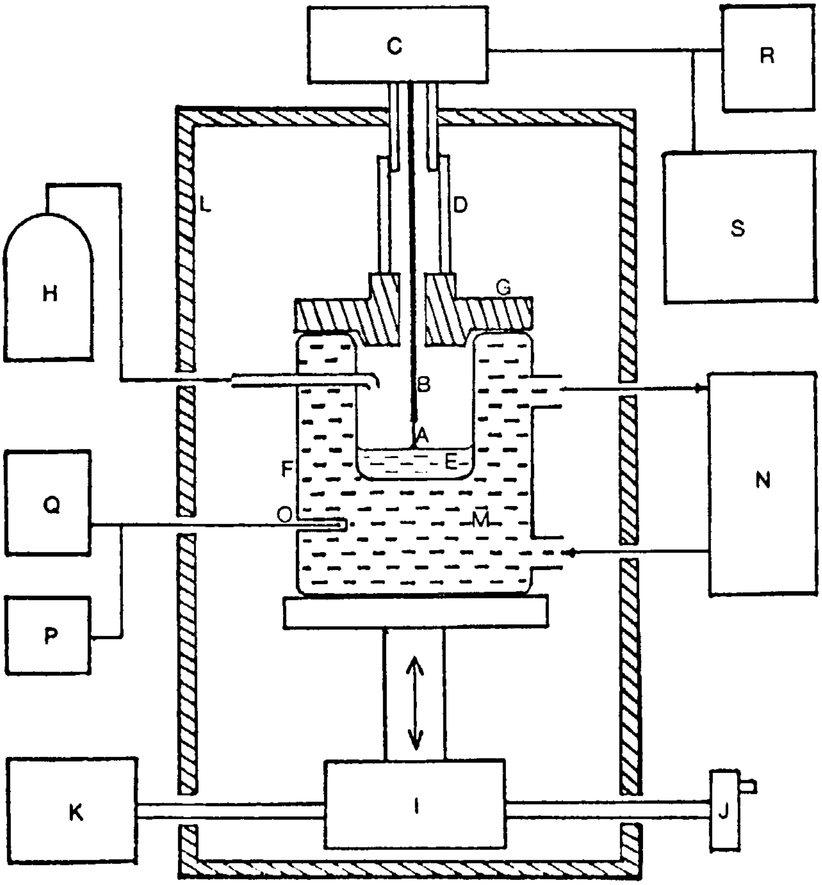

FIGURE 1 A schematic diagram of the experimental set-up for the Wilhelmy balance experiment.

A: Measured Fibre
B: Glass Rod
C: Electro-Balance
D: Glass Sleeve
E: Liquid
F: Double-Walled Glass Cell
G: Teflon Lid
H: Argon Cylinder
I: Movable Platform
J: Hand-Dial
K: Motor-Drive Mechanism
L: Enclosed Cabinet
M: Thermostat Water
N: Temperature Control Bath
O: Thermocouple
P: Ice-Point Reference
Q: Digital Voltmeter
R: Digital Voltmeter
S: X-Y Recorder

of the glass rod was used to cover the measuring cell so that evaporation of the liquid could be mimimized. Furthermore, argon (H) was continually percolated through the measuring cell to create an inert atmosphere. The measuring cell was then mounted on a movable platform (I) which could be raised or lowered either by a hand-dial (J) or a motor-drive mechanism (K). The complete set-up is enclosed in a cabinet (L) with a transparent plexiglass door to facilitate observations.

The temperature in the measuring cell was controlled by the circulation of thermostat water (M) from a temperature control bath (N). The temperature inside the measuring cell was detected by a thermocouple (O). With the thermocouple and an ice-point temperature reference (P), the temperature could be read by means of a digital voltmeter (Q). The output of the electro-balance, in the form of voltage, was recorded by a digital voltmeter (R) and an x-y chart-recorder (S).

Because of the small weight changes during the measurements, the output of the electro-balance was easily affected by any electronic noise or mechanical vibration. In order to minimize the vibration effects, the complete set-up was mounted onto a heavy table. Also, the electronic background noise was reduced by grounding all electronic instruments appropriately and using shielded wires for all connections.

From Eq. (1), to calculate the contact angle accurately, the precise value for the perimeter of the fibre has to be known. The perimeter of the fibre was obtained precisely by first dipping the fibre into a liquid which was known to wet the fibre completely. Under the complete wetting condition, the 'cos θ' term in Eq. (1) could be set equal to 1, thus the perimeter, p, is:

$$p = \frac{F}{\gamma_{LV}} \qquad (2)$$

Since the surface tensions of the two measured fibres, Thornel 300 and Kevlar were expected to have surface properties close to common polymers, a liquid with low surface tension should wet the fibres completely. Toluene, which has a surface tension of 28.4 mJ/m^2 at 24°C, was chosen. It was found that the diameters of the carbon fibres were rather uniform from one fibre to another. They ranged from 6.8 to 8.0 μm. The diameters of the Kevlar, which ranged from 10.8 to 13.4 μm, seemed to have a wider variation between fibres. The fibre diameter was further checked by using a Digital Image Analysis System (Bausch and Lomb Omnicon 3000).

After finding the perimeter of the fibre, a measuring liquid (water, ethylene glycol or glycerol) was put into the double-walled glass cell. By controlling the movement of the platform with the controllable speed motor, advancing contact angle measurements were obtained by immersing the fibre into the liquid slowly. Figure 2 shows the resultant weight changes recorded during the experiment. The motor, which was used to dip the fibre into the liquid, was stopped after the fibre and the liquid had come into contact. The system was then allowed a few seconds to stabilize. Readings of the equilibrium force output for the next few seconds were recorded on the x-y chart recorder. In order to generate more data, the fibre was then immersed further into the liquid (as indicated by the tag marks in Figure 2) to set up another three-phase line and then stopped to take a second reading. Since the

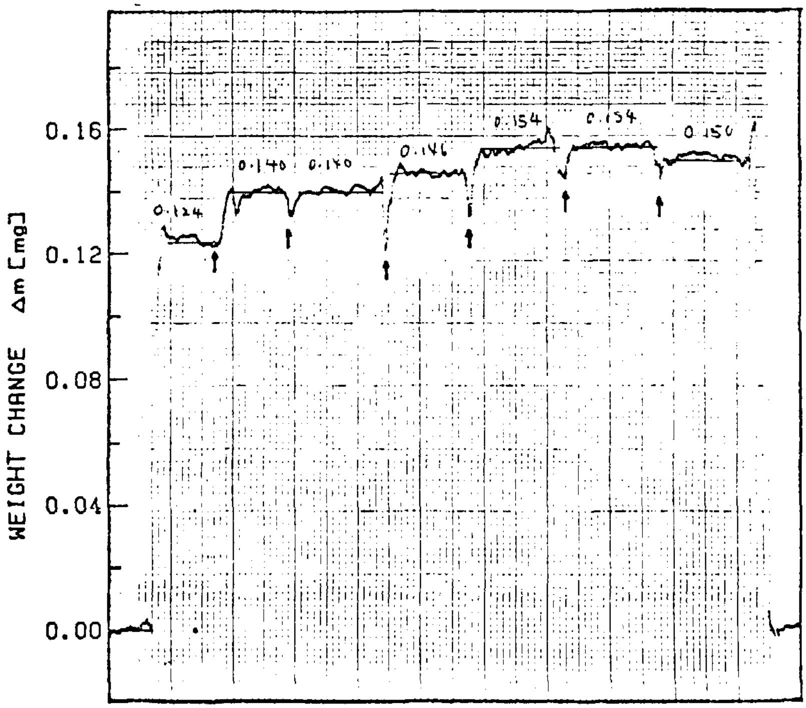

FIGURE 2 Static weight change with a Kevlar® fibre in water.

fibre diameter is so small, the buoyancy effect is negligible. The average of all these readings was used to calculate the advancing static contact angle.

The solidification front method

The behaviour of small particles at slowly advancing solidification fronts is expected to be governed by thermodynamic effects. The decisive step in particle ingestion from the liquid to the solid phase is particle adhesion to the solid/liquid interface. Therefore this process is expected to be governed by the free energy of adhesion:

$$\Delta F^{adh} = \gamma_{PS} - \gamma_{PL} - \gamma_{SL} \tag{3}$$

where γ_{PS}, γ_{PL} and γ_{SL} are the interfacial tensions of the particle-solid interface, the particle-liquid interface and the solid-liquid interface, respectively. If this ΔF^{adh} is positive, the thermodynamic prediction is repulsion. However, it has been shown that at higher solidification rates, a viscous drage force is generated which opposes the thermodynamic repulsive force.[10] The solidification front velocity at which the viscous drag force is balanced by the thermodynamic repulsive force, and thus engulfment of the particle is observed, is called the critical velocity. An equation has been derived to relate the critical velocity to the ΔF^{adh} of a system.[10-14]

$$\Delta F^{adh} = 6070 \left[\frac{\rho_L^{0.685} T_{mp}^{0.400}}{\mu^{0.085}}\right] \left[\frac{k_p^{0.601}}{(\rho_p C_p)^{0.201}}\right] D^{0.484} V_c^{0.085} \tag{4}$$

where

ΔF^{adh} = Free energy of adhesion; mJ/m^2;
ρ_L = Density of matrix liquid phase; kg/m^3;
T_{mp} = Matrix material melting temperature; K;
μ = Absolute viscosity of matrix liquid phase; Ns/m^2;
k_p = Thermal conductivity of particle; W/(m.K);
ρ_p = Density of particle; kg/m^3;
C_p = Specific heat of particle; J/(kg.K);
D = Equivalent spherical diameter; m;
V_c = Critical velocity of engulfing; m/s.

Thus ΔF^{adh} can be calculated from the experimentally obtained critical velocity.

In addition, there exists an equation of state for interfacial tensions which states that γ_{13} is a known function of γ_{12} and γ_{23}[15]. Therefore, Eq. (3) can be written as

$$\Delta F^{adh} = f(\gamma_{SV'}\gamma_{PV}) - f(\gamma_{PV'}\gamma_{LV}) - f(\gamma_{SV'}\gamma_{LV}) \qquad (5)$$

If γ_{SV} and γ_{LV} of the matrix material are known, the particle surface tension, $\gamma_{PV'}$ can be calculated from the value of ΔF^{adh}. The technique has been applied successfully to determine the surface tension of a wide variety of particles, such as polymer particles,[14] coal particles,[16] and biological cells.[17]

Experimental

The fibres were first chopped into small segments from 10 to 300 μm in length and then put into a copper chamber of about 3 mm depth. A 20 × 60 mm glass slide was used to cover this chamber.[18] After melting the matrix material, a very thin layer of the particle matrix suspension was formed. Two thermoelectric devices mounted under the two ends of the copper cell were used for heating and cooling the cell. A cooling water channel under the thermoelectric devices was used to dissipate the excess heat. The temperatures at the two ends, T_1 and T_2, were detected by two thermistors. A constant temperature gradient was set up by maintaining the temperature difference ($T_1 - T_2$) by means of two bipolar controllers and a feedback control temperature programmer. By lowering T_1 and T_2 at the same rate, the front moved horizontally in the copper chamber. The behaviour of the fibres at the solidification front was then observed through a microscope. The size of the fibre and the solidification rate were measured by a calibrated eyepiece graticule and a stop watch. At higher velocities, the process could be videotaped and analyzed during slow-motion playback.

At low solidification front velocities, the fibres always lined up with the front and were then pushed further along. Such observations were considered to be rejection. Sometimes, after being pushed for a small distance (less than 30.4 μm or 2 grids on the eyepiece graticule of the microscope), they were engulfed by the advancing front. Since it was not certain whether these cases were engulfments or rejections, they were recorded as 'transition'. If the fibre was engulfed immediately after it had lined up with the front, it was taken as "engulfment". The observations were then plotted on a graph of solidification front velocity versus fibre length as in Figures 3 to 5. The upper limit of the

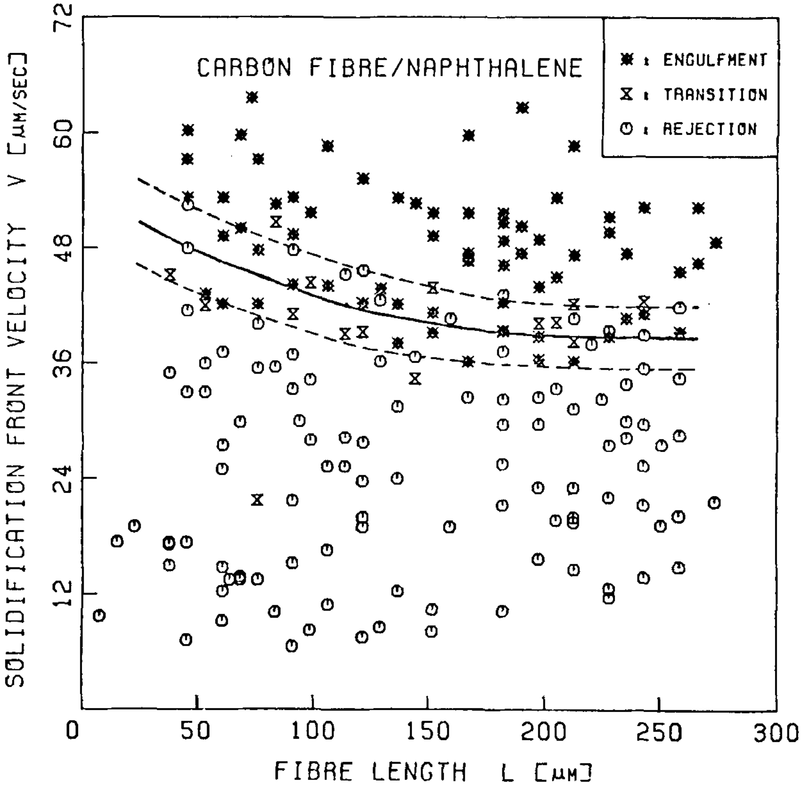

FIGURE 3 Solidification front velocity, V, of naphthalene versus carbon fibre length, L.

critical velocity was taken as the line above which all the fibre particles were engulfed and the lower limit was taken as that below which all the fibre particles were rejected. The average between these two limits was taken as the mean critical velocity.

RESULTS

A. Wilhelmy balance method

The weight change results, such as in Figure 2, were used to calculate the contact angles of three different liquids on the fibres. The results are listed in Table 1. With the use of the equation of state,[15] γ_{SL} can

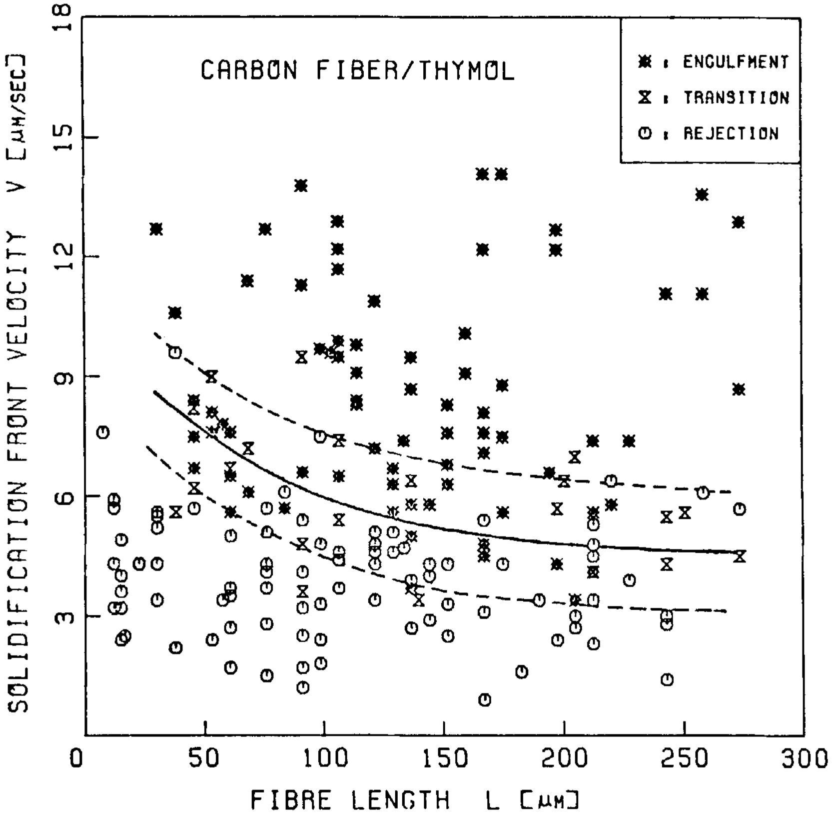

FIGURE 4 Solidification front velocity, V, of thymol versus carbon fibre length, L.

be expressed as a function of γ_{SV} and γ_{LV}, *i.e.*

$$\gamma_{SL} = f(\gamma_{SV}, \gamma_{LV}) \tag{6}$$

Together with Young's equation,[19]

$$\gamma_{SV} - \gamma_{SL} = \gamma_{LV} \cos\theta \tag{7}$$

it was thus possible to evaluate the fibre surface tension γ_{SV} from knowing the liquid surface tension and the contact angle. The average surface tension of the carbon fibre was found to be 42.4 mJ/m^2 and that for the Kevlar was 43.7 mJ/m^2 at 24°C, as summarized in Table 1.

Using the Superposition of Error Theorems and taking into account

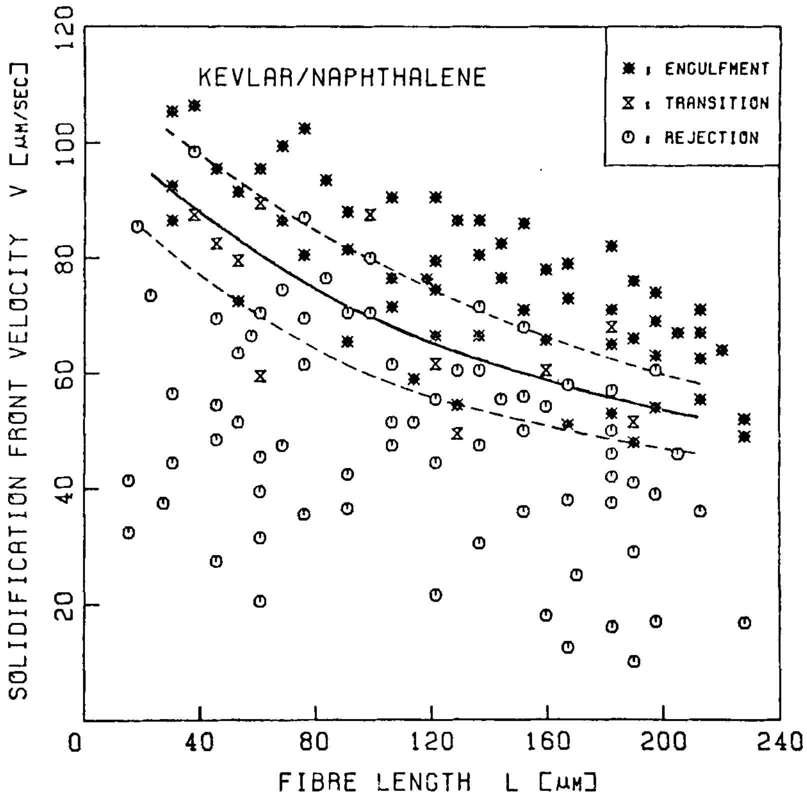

FIGURE 5 Solidification front velocity, V, of naphthalene versus Kevlar® fibre length, L.

the errors in the electrobalance output, the liquid surface tensions and the fibre perimeter measurements, the error limits of the results were estimated[20] and recorded in Table 1.

B. Solidification front method

The mean critical velocities at various fibre lengths were obtained from the observation graphs, such as Figures 3 to 5. The effective diameter of the fibre was taken as the diameter of a sphere with equivalent projected area. In order to use Eq. (4) for calculating ΔF^{adh}, certain physical properties of the matrix and the particle material have to be known. The values for the densities, melting temperatures and vis-

TABLE I

The static advancing contact angle, θ_a of various liquids on carbon and Kevlar® fibres and the surface tension, γ_{PV} of the fibres

Fibre	Liquid	θ_a (Degrees)	γ_{PV} (mJ/m^2)
Carbon	Ethylene Glycol	31.2±8.8	41.6±3.2
Carbon	Glycerol	55.7±3.6	42.2±1.6
Carbon	Water	66.0±2.6	43.3±1.5
Kevlar	Ethylene Glycol	27.8±5.7	42.8±2.0
Kevlar	Glycerol	52.8±2.7	43.8±1.6
Kevlar	Water	63.8±1.5	44.6±0.9

TABLE II

Physical properties of the organic materials at their respective melting temperatures[8-10]

Matrix material	Melting temperature T_{mp} (K)	Density ρ(kg/m^2)	Viscosity μ(Ns/m^2)	γ_{SV} (mJ/m^2)	γ_{LV} (mJ/m^2)
Benzophenone	321	958.3	0.00515	34.5	39.9
Thymol	324.5	925	0.00397	29.4	29.9
Naphthalene	353	978	0.000967	22.9	32.8

TABLE III

The critical velocities, V_c and free energy of adhesion, ΔF^{adh} of carbon and Kevlar® fibres as a function of fibre length in various matrix materials

		V_c (μm/sec)		ΔF^{adh} x FP(mJ/m^2)	
Matrix material	Fibre length	Carbon fibre	Kevlar fibre	Carbon fibre	Kevlar fibre
Thymol	50	6.9	3.77	16.9	12.6
	100	5.4	3.02	16.9	12.8
	150	4.7	2.30	16.8	11.7
	200	4.4	2.08	17.4	11.7
Benzophenone	50	2.12	18.1	7.5	36.8
	100	1.91	15.4	8.2	38.9
	150	1.81	13.8	8.7	39.8
	200	1.76	13.2	9.2	41.4
Naphthalene	50	47.2	88.7	76.4	132.7
	100	43.3	70.8	85.2	134.5
	150	41.0	61.5	90.5	134.7
	200	39.4	52.6	94.5	129.9

cosities for the matrix materials, as summarized in Table 2, have been established.[11-13] Also, the data for the density, specific heat capacity and thermal conductivity of the carbon fibre have been compiled by

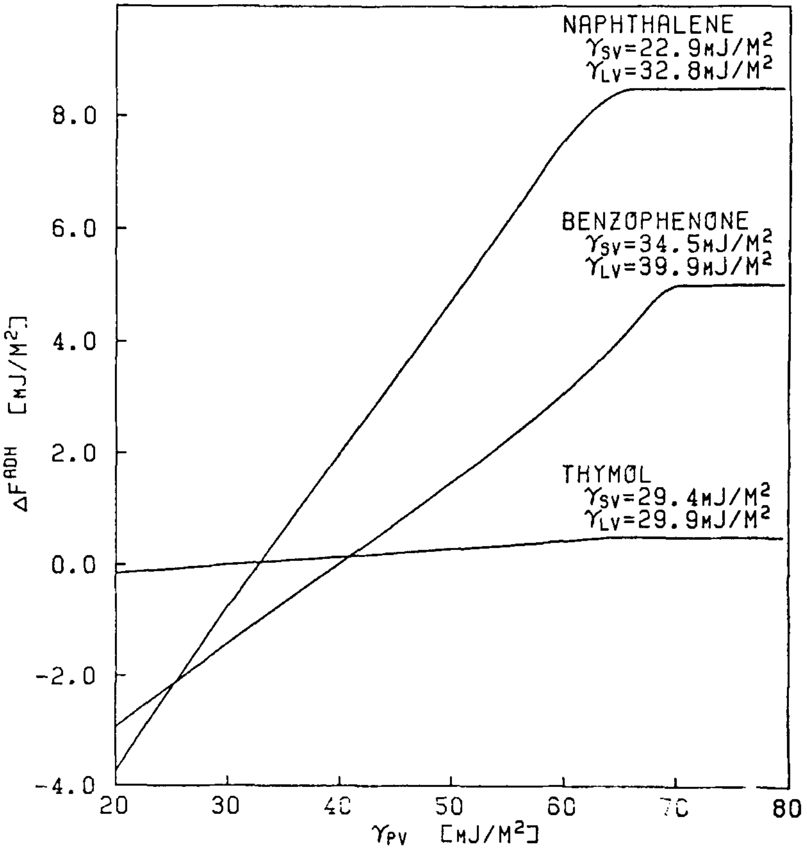

FIGURE 6 The change in the free energy of adhesion, ΔF^{adh}, as a function of particle surface tension, γ_{PV}, in different matrix materials.

the manufacturer. However, when putting these values into the empirical equation, the ΔF^{adh} obtained was unrealistically high. This occurred because the empirical equation was calibrated by using particles with very low thermal conductivities compared to those of the carbon fibres. Furthermore, the physical properties of the Kevlar were not available. In view of all these difficulties, it was then decided to keep the expression $\frac{k_p^{0.601}}{(\rho_p C_p)^{0.201}}$ in Eq. (4) as a fibre property term (FP) in the calculation of ΔF^{adh}. The ΔF^{adh} then calculated were expressed as a function of FP. The critical velocities as well as the ΔF^{adh} of the carbon and Kevlar fibres as a function of fibre length in various matrix materials are shown in Table 3.

With the use of the equation of state, the ΔF^{adh} of particles in a particular solid/liquid matrix for which γ_{LV} and γ_{SV} are known is a function of the particle surface tension, γ_{PV}, only. Figure 6 was produced using the equation of state to calculate ΔF^{adh} as a function of γ_{PV}, for the three matrix materials with known surface tensions γ_{LV} and γ_{SV}. It is noticed in Figure 6 that there is an almost linear relation between ΔF^{adh} and γ_{PV} before the plateau region, where the slope of these plots becomes zero. Linear regression tests were performed on this region before the plateau on the three curves in Figure 6. To relate the result back to a room temperature of 24°C a value of $\delta\gamma_{PV}/\delta T = -0.1$ mJ/m²°C was chosen. This value is typical for both liquids and solids[21], and deviations from this value by more than 50% are rare. It was found that

$$\gamma_{PV} = 31.7\ \mathrm{mJ/m^2} + 72.6\ \Delta F^{adh} \tag{8}$$

for thymol,

$$\gamma_{PV} = 41.5\ \mathrm{mJ/m^2} + 6.92\ \Delta F^{adh} \tag{9}$$

for benzophenone, and

$$\gamma_{PV} = 36.5\ \mathrm{mJ/m^2} + 3.67\ \Delta F^{adh} \tag{10}$$

for naphthalene.

Inserting ΔF^{adh} calculated by Eq. (4) and listed in Table 3 into the corresponding equations, Eqs. (8)–(10), there are only two unknowns left, γ_{PV} and FP. Since both of these values are properties of the fibre only, they can be solved by coupling a pair of equations from the three matrix systems. Table 4 shows a calculated result in

TABLE IV

Surface tension, γ_{PV} of carbon fibre calculated by using ΔF^{adh} in thymol and benzophenone

Fibre length (μm)	ΔF^{adh} in thymol x FP(mJ/m²)	ΔF^{adh} in benzophenone x FP(mJ/m²)	γ_{PV} (mJ/m²)
50	16.9	7.5	41.9
100	16.9	8.2	42.0
150	16.8	8.7	42.0
200	17.4	9.2	42.0

TABLE V

Summary of the surface tensions, γ_{PV} of the fibres obtained by coupling the ΔF^{adh} of pairs of systems

Pair of matrices used	γ_{PV} (mJ/m^2) carbon fibre	Kevlar®
Thymol/benzophenone	42.0	46.6
Benzophenone/naphthalene	43.2	47.3
Thymol/naphthalene	40.3	45.3
Average:	41.8	46.4

TABLE VI

Summary of the contact angles, θ and surface tensions, γ_{PV} obtained by the Wilhelmy balance technique and the solidification front technique

	Wilhelmy balance technique			Solidification front technique		
Fibre	θ (Degrees) with water	θ (Degrees) with glycerol	γ_{PV} (mJ/M^2)	θ (Degrees) with water	θ (Degrees) with glycerol	γ_{PV} (mJ/m^2)
Carbon	68.4	50.8	42.4	68.9	51.2	41.8
Kevlar	66.2	49.0	43.7	61.2	45.1	46.4

which the surface tension of carbon fibre was calculated by using the ΔF^{adh} measurements in thymol and benzophenone. As one might expect, the surface tension of the fibre does not depend on the fibre length. This result further proves the consistency of the empirical equation, Eq. (4). Similar calculations were done with each pair of the three matrix systems for the two types of fibres. The results are summarized in Table 5. The average surface tensions of the carbon fibre and the Kevlar were found to be 41.8 mJ/m^2 and 46.4 mJ/m^2 at 24°C respectively. An error analysis was performed by taking into consideration the error in critical velocity, which was taken as the critical velocity band as shown in Figures 3–5. It was found that the error limits for the results where thymol was used as a matrix material were about ± 1.5 mJ/m^2 while for those results where thymol was not used as one of the matrices the errors were substantially lower, between 0.1 and 0.7 mJ/m^2.

DISCUSSION

A comparison of the results obtained using the Wilhelmy technique and the solidification front technique is shown in Table 6. The contact angles and surface tensions determined for the carbon fibres are essentially the same, regardless of technique. For the Kevlar fibres there is a somewhat larger discrepancy in the results obtained by the two techniques. Overall, the comparison of results illustrates that both techniques will produce reliable surface tension and contact angle data for small diameter fibres.

Furthermore, error analysis for the Wilhelmy technique has indicated that the largest error limit in surface tension results in Table 1 is ± 3.2 mJ/m^2 in the carbon fibre/ethylene glycol experiment, while the error limits in all other experiments are around ± 1 to ± 2 mJ/m^2. The error analysis has indicated that the choice of liquid used for the Wilhelmy balance measurements is very important. The mass changes recorded by the electrobalance for a given fibre using the different liquids were of the same order of magnitude. In fact, the mass changes recorded using ethylene glycol were on average larger than the mass changes obtained with water and glycerol. Thus, the relative error in the mass readings for ethylene glycol would be expected to be less than, or at worst equal to, the errors produced from measurements performed with the other liquids. Therefore, the relatively large errors in the calculated contact angle and surface tension values obtained from the ethylene glycol measurements are due to the calculations, not the original measurements. For example, larger errors are generated in some calculations as opposed to others due to the non-linearity of the cosine function. For a high $\cos\theta$ value, such as $\cos\theta = 0.9$, a 0.01 imprecision will induce a $\pm 1.3^\circ$ error in the contact angle; while at $\cos\theta = 0.2$, the error induced by the same 0.01 imprecision is only $\pm 0.5^\circ$. Thus, liquids which generate a contact angle on the fibres closer to 90° are preferred.

With respect to the solidification front technique, it is seen in Figure 6 that the change in ΔF^{adh} due to changes in γ_{PV} varies with the matrix material. In the case of thymol, which is a matrix where γ_{SV} and γ_{LV} are very close in value, changes in γ_{PV} result in smaller changes in ΔF^{adh} than in the case of the matrix materials benzophenone and naphthalene. This means a change in the particle surface tension will have a smaller effect on the critical velocity in thymol than in other matrix materials. It also gives rise to the higher error limits in calculating the surface tension of the particle. Therefore, in order to achieve higher accuracy, the use of benzophenone and naphthalene for the solidification front experiments is preferable.

Although both techniques used in this investigation were found to be satisfactory in measuring the surface tensions and contact angles of small diameter fibres, complications could arise with other fibrous materials. For instance, in the Wilhelmy balance experiment, it is not possible to measure the fibre diameter and the contact angle simultaneously; also, finding the correct perimeter of a less uniform fibre might be difficult. The fibre geometry is also very important; for example, a convoluted cross section would generate a wicking effect and thus give incorrect balance readings. Furthermore, a rough fibre surface would result in large contact angle hysteresis and the possibility of obtaining an incorrect contact angle measurement is thus more likely. Since the Kevlar fibres used in this investigation have a rougher surface than the carbon fibres, it would be expected that the solidification front experiments give a more reliable result than the Wilhelmy balance method as far as γ_{PV} is concerned. As for the solidification front method, there are fewer limitations. Also, the consistency and reproducibility shown in different matrix systems provide credence to the technique. Further refinement of this technique is feasible. Such developments could include tests with fibres having a wider range of surface tension to check the generality of this work. Complete automation of the experiment is also possible, in principle, through the use of digital image analysis.

In conclusion, it should be restated that both the Wilhelmy balance method and the solidification front method are very useful in determining wettability and surface tension of thin fibres. The solidification front technique, not used heretofore for this purpose, offers some significant advantages.

References

1. M. E. Schrader, in *Surface Characteristics of Fibers and Textiles*, M. J. Schick, Ed. (Marcel Dekker, New York, 1977), p. 525.
2. L. H. Sharpe and H. Schonhorn, in *Contact Angle, Wettability and Adhesion, Advances in Chemistry Series, Vol. 43* (ACS, Washington, D.C., 1964), p. 189.
3. J. R. Huntsberger, *J. Adhesion* **12**, 3 (1981).
4. W. A. Zisman, in *Symposium on Adhesion and Cohesion*, P. Weiss, Ed. (Elsevier, New York, 1962).
5. A. W. Neumann and W. Tanner. *Vth Intern. Congress Surface Acitivity*, Barcelona, 1968, Vol. 2, p. 727.
6. B. Miller, and R. A. Young, *Textile Research Journal*, **45**, 359–365 (1975).
7. B. Miller, in *Surface Characteristics of Fibres and Textiles*, M. J. Schick, Ed. (Marcel Dekker Inc., New York 1977), p. 417–445.
8. S. Hedvat, Ph.D. thesis in Chemical Engineering, Princeton University, Princeton, New Jersey (1981).

9. A. W. Neumann and R. J. Good, in *Surface and Colloid Science, Vol. 11*, R. J. Good and R. R. Stromberg, Eds. (Plenum Press, New York, 1979), p. 31.
10. S. N. Omenyi, Ph.D. Thesis, University of Toronto (1979).
11. R. P. Smith, M.A.Sc. Thesis, University of Toronto (1981).
12. S. N. Omenyi, A. W. Neumann, C. J. van Oss, *J. Appl. Phys.* **52**, 789 (1981).
13. S. N. Omenyi, *et al., J. Appl. Phys.* **52**, 796 (1981).
14. S. N. Omenyi, R. P. Smith, A. W. Neumann, *J. Colloid Interface Sci.* **75**, 117 (1980).
15. A. W. Neumann, *et al., J. Colloid Interface Sci.* **49**, 291 (1974).
16. M. R. Soulard, E. I. Vargha-Butler, A. W. Neumann, *54th Colloid and Surface Science Symposium*, Lehigh University (1981).
17. J. K. Spelt, *et al., Cell Biophysics* **4**, 117 (1982).
18. D. W. Francis, Ph.D. Thesis, University of Toronto (1983).
19. T. Young, *Phil. Trans. Roy. Soc.* **95**, 65 (1805).
20. S. K. Li, M.A.Sc. Thesis, University of Toronto (1983).
21. S. N. Omenyi, A. W. Neumann, *J. Appl. Phys.* **47**, 3956 (1976).